COMPUTATIONAL STUDY OF INCOMPRESSIBLE FLOW BY FINITE-DIFFERENCE METHOD

Kunio Kuwahara
Institute of Space and Astronautical Science
Yoshinodai, Sagamihara, Kanagawa, Japan

Incompressible high-Reynolds-number flows are simulated by solving the Navier-Stokes equations. A finite-difference method with third-order upwinding are employed without using any turbulence model. Validity of this method is discussed.

Also, a newly developed multi-directional formulation is applied for improved accuracy. Examples are presented to show the applicability of the present approach to variety of problems.

INTRODUCTION

Many of the high-Reynolds-number, turbulence simulations have been based on Reynolds-averaged Navier-Stokes equations using a turbulence model. Some use a large-eddy simulation based on a Smagorinsky-type model. However, a turbulence model or a large-eddy simulation is not suitable for high-Reynolds-number-flow computation because, there, the effect of turbulence mixing is usually replaced by second-order diffusion. This diffusion is similar to viscous diffusion. It means that we are simply computing a locally low-Reynolds-number flow.

There are some real direct numerical simulation in which most of the small-scale structure are resolved, but the computations can be done only at relatively small Reynolds numbers. It demands too much computer resources. We can not use enough grid points for high-Reynolds-number flows of practical interest. We have rather to use a very coarse grid system. In many applications, large structures are most important and we are not interested much about in small structures. What we want to do is to capture the large-scale structure using a coarse grid system.

On the other hand, quit a few simulations (see Kuwahara, 1992), show that large structures of high-Reynolds-number, turbulent flow can be captured using relatively coarse grid, if the numerical instability, usually unavoidable for high-Reynolds-number-flow simulation, is suppressed. Most successful simulations in these approaches are based on the third-order upwind formulation (Kawamura and Kuwahara, 1984). An approach similar in philosophy but different in method is adopted by Boris et. al. (1992).

In the present paper, we summarize the third-order upwind scheme for high-Reynolds-number-flow computations. To increase the accuracy, we have developed a new finite-difference scheme named as multi-directional finite-difference method. Most of the results in the present paper is based on this new scheme.

Following examples are presented in this paper to show the validity of the approach.

0) One-dimensional Burgers turbulence.
1) Two-dimensional flow around a circular cylinder at the Reynolds numbers from 0.1 to 1000000.
2) Three-dimensional transitional flow in a square channel at Reynolds numbers 12500.
3) Three-dimensional flow around a car at Reynolds number 1000000.
4) Three-dimensional thermal convection in a box at Rayleigh number 17000000..

COMPUTATIONAL METHOD

The governing equations are the unsteady incompressible Navier-Stokes equations and the equation of continuity as follows:

$$divu = 0 \tag{1}$$

$$\frac{\partial u}{\partial t} + u \cdot gradu = -gradp + \frac{1}{\mathrm{Re}}\Delta u \tag{2}$$

where u, p, t and Re denote the velocity vector, pressure, time and the Reynolds number respectively. For high-Reynolds-number flows, time-dependent computations are required owing to the strong unsteadiness. These equations are solved by a finite-difference method. The numerical procedure is based on the MAC method. The pressure field is obtained by solving the following Poisson equation:

$$\Delta p = -div(u \cdot gradu) + \frac{D^n}{\delta t} \tag{3}$$

$$D = divu \tag{4}$$

where n is the time step and δt is the time increment. D^{n+1} is assumed to be zero, but D^n is retained as a corrective term.

In cases 1, 2, 4, a generalized coordinates system is employed, so that enough grid points can be concentrated near the body surface where the no-slip condition is imposed.

All the spatial derivative terms are represented by the central difference approximation except for the convection terms. For the convection terms, the third-order upwind difference is used. This is the most important point for high-Reynolds-number computations and the detail is given below.

Strong numerical instability caused by the aliasing error occurs at high Reynolds numbers, owing to the non-linear convection terms, if enough grid points are not used to resolve the small-scale structures. When digitizing a continuous function into a finite number of the values, it is very important to filter out the high-frequency part of the original function which can not be resolved by the digital system. If not, aliasing error makes the approximation meaningless.

Usually a turbulence model or a large eddy simulation is used to get rid of this instability. The diffusion coefficients increased by the added turbulent viscosity reduce the aliasing error and suppress the numerical instability. In most of the models ,this diffusion has the same form as the viscous diffusion and the diffusion coefficient is usually much larger than that of the viscous diffusion. Therefore, the effect of physical diffusion is concealed, resulting no dependency of the flow on the Reynolds number is captured.

Another way to stabilize the computation is to use an upwind scheme. The first-order upwind scheme is widely used because of the very good stability but the leading numerical error caused by this upwinding is second order and similar to the physical diffusion. This should be avoided because of the same reason just mentioned above

The second-order upwind scheme has a dispersion type leading error, which makes the computation unstable generally.

For the discretization of the non-linear convection terms, the order of accuracy is odd or even has special importance for stable computation. In case of even order of accuracy, the leading numerical-error term is the odd-order derivative which is dispersive. Once some error is created, the error never diffuses but moves around in the computational domain until the computation blows up. Eventually no stable solution can be obtained in this case. On the other hand, in case of odd order of accuracy, the leading error term is the even-order derivative which is diffusive. This makes the computation very stable by reducing the aliasing error well.

A third-order upwind scheme has been found to be most suitable for high-Reynolds-number-flow computation. The leading numerical error terms are the fourth-order derivative terms, where the effects of the second-order numerical diffusions are carefully removed. The numerical diffusion of forth-order derivatives is of short range and does not conceal the effect of molecular diffusion but well stabilizes the computation.

One simple explanation why the fourth-order diffusion does not conceal the effect of second-order diffusion is as follows. A finite-difference representation of the fourth-order diffusion term is as follows:

$$(u_{i+2} - 4u_{i+1} + 6u_i - 4u_{i-1} + u_{i-2}) / \partial x^4 \tag{5}$$

This can be written as ,

$$4\delta x^2 \left(\frac{u_{i+2} - 2u_i + u_{i-2}}{(2\delta x)^2} - \frac{u_{i+1} - 2u_i + u_{i-1}}{\delta x^2} \right) \tag{6}$$

The two terms in Eq.6 represent the second-order diffusion and their effects cancel each other except near the point i. This means fourth-order diffusion is very independent from second-order diffusion. In general, the effects of lower-order diffusion are not concealed by higher-order diffusion.

Similarly, fifth-order upwinding is possible and some computations have been done but it requires seven points in each direction to approximate the local derivative. This means to require a wider range of analyticity to the solution of the equations. High-Reynolds-number flows are not so analytical, therefore it is not necessarily better than third-order unwinding.

There are several third-order upwind schemes. We use the following scheme. Initially, the one-sided second-order finite difference approximation is employed for the convection terms.

$$u\frac{\partial u}{\partial x} = u_i \left(\frac{3u_i - 4u_{i-1} + u_{i-2}}{2\delta x} \right), u_i > 0 \tag{7}$$

$$u\frac{\partial u}{\partial x} = u_i \left(\frac{-3u_i + 4u_{i-1} - u_{i-2}}{2\delta x} \right), u_i \le 0 \tag{8}$$

We can rewrite the above equations to a symmetrical form as follows:

$$\begin{aligned} u\frac{\partial u}{\partial x} &= u_i(-u_{i+2} + 4(u_{i+1} - u_{i-1}) + u_{i-2}) / 4\partial x \\ &+ |u_i|(u_{i+2} - 4u_{i+1} + 6u_i - 4u_{i-1} + u_{i-2}) / 4\partial x \end{aligned} \tag{9}$$

If the first term of Eq.(9) is developed into Taylor series, it becomes

$$u\frac{\partial u}{\partial x} - \frac{1}{3}\delta x^2 u\frac{\delta^3 u}{\partial x^3} + O(\delta x^4) \tag{10}$$

Similarly the second term becomes

$$\delta x^3 u\frac{\delta^4 u}{\partial x^4} + O(\delta x^5) \tag{11}$$

Therefore, the leading error of Eq.(9)is order δx^3 and its coefficient includes third-order derivative. As mentioned above, odd order-derivative is not desirable, but this error term is eliminated if the term is replaced by

$$|u_i|(-u_{i+2} + 8(u_{i+1} - u_{i-1}) + u_{i-2}) / 12\partial x \tag{12}$$

As a result, the present third-order upwind scheme is represented by five grid points as follows:

$$\begin{aligned} u\frac{\partial u}{\partial x} &= u_i(-u_{i+2} + 8(u_{i+1} - u_{i-1}) + u_{i-2}) / 12\partial x \\ &+ |u_i|(u_{i+2} - 4u_{i+1} + 6u_i - 4u_{i-1} + u_{i-2}) / 4\partial x \end{aligned} \tag{13}$$

There is another version of third order upwind schemes for example as follows.

$$\begin{aligned} u\frac{\partial u}{\partial x} &= u_i(-u_{i+2} + 8(u_{i+1} - u_{i-1}) + u_{i-2}) / 12\partial x \\ &+ \alpha|u_i|(u_{i+2} - 4u_{i+1} + 6u_i - 4u_{i-1} + u_{i-2}) / 4\partial x \end{aligned} \tag{14}$$

where $\alpha = 1/3$ is called UTOPIA scheme by Leonard. We compared these schemes and as well as QUICK scheme by comparing the energy spectrum in one-dimensional Burgers turbulence and found the above Kawamura-Kuwahara scheme is the best (Fig.1). When we use a very fine grid as 4096 points, the three scheme agrees completely with each other and theoretical prediction. However, with reducing the number of grid points, the difference become clear. Only the present method give the good agreement with the result of very fine computations. For the theoretical validation based on the digital-filter theory has been given by Hashiguchi (1997).

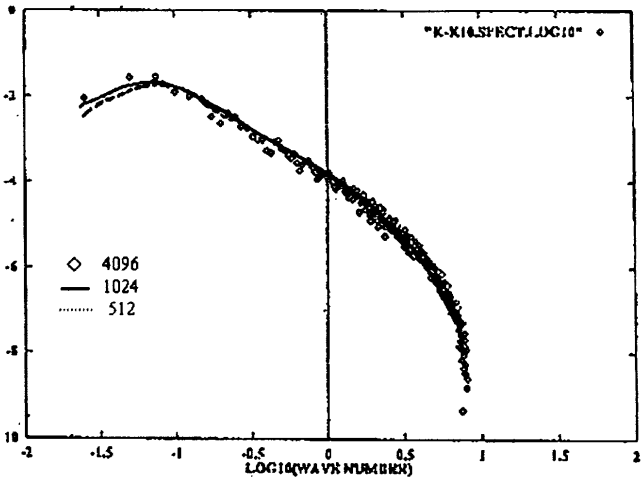

(a) The present scheme (Kawamura-Kuwahara)

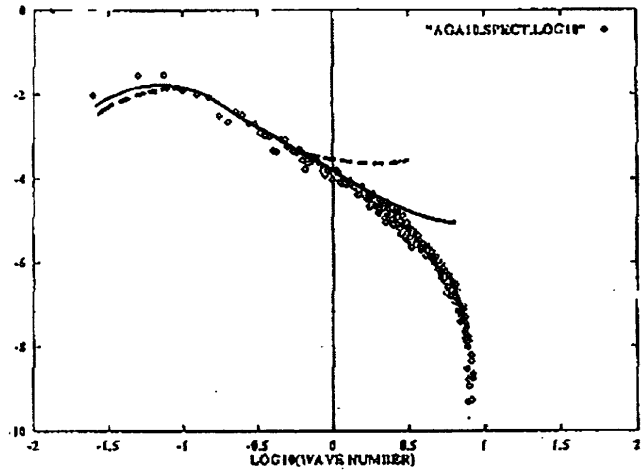

(b)UTOPIA

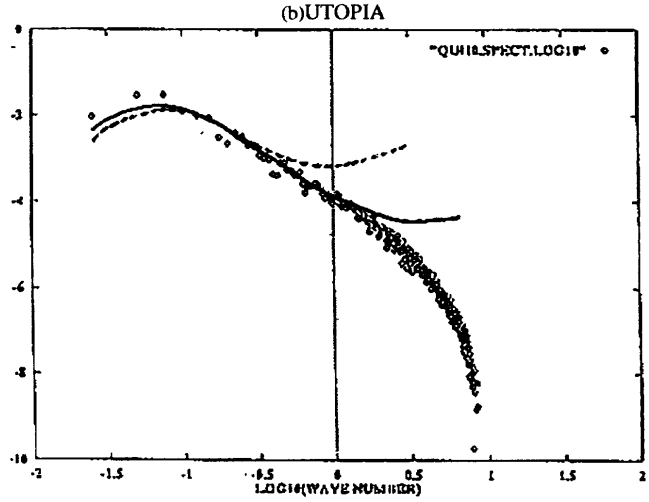

(c) QUICK

Fig.1 Energy specrtum for Burgers turbulence

There is another important problem in high-order upwind schemes. That is, the accuracy decreases when the flow direction is not well parallel to one of the coordinate lines. If we use generalized coordinate system, near the boundary, the flow direction and one of the coordinate lines are almost parallel, and this problem is not serious. However, in general, flow direction is not always parallel to a coordinate line and the problem become very important

To overcome this problem we introduced the multi-directional upwind method. This method is summarized as follows;

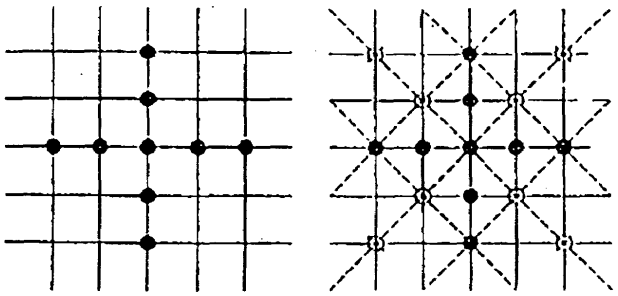

(a) system A (b) system B
Fig.2 Grid for multi-directional scheme

When structured grid points are given, the black points in Fig.2-a are usually used to approximate the derivatives at the central point (system A).

If we introduce the other 45 degrees-rotated local grid points, the white ones in Fig.2-b, which can be used to approximate the derivatives at the central point (system B).

In order to improve the derivative value at the central point, we mix the derivative values calculated from both systems (A and B) at a proper ratio. We adopt the ratio A : B = 2/3 : 1/3. Using this ratio, for example, resulting finite-difference scheme for the Laplacian coincides with the well-known 9-points formula with forth-order accuracy. This method improves the rotational invariance of the coordinate system. Then those flows where flow direction is not parallel to the grid direction are better simulated.

For all the spatial derivatives, the multi-directional finite-difference method is used. This method has another advantage. In MAC method, usually staggered mesh is used to remove the unphysical oscillation of the pressure. This oscillations is caused by the decoupling of the computed values within the nearest two points. These values couples more tightly with the second nearest points. This decoupling become less if we use third-order upwind scheme because of the five-point differencing, but there remains some. However, if we use multi-directional finite-difference method, every point becomes tightly coupled and the oscillation disappears. Therefore, a non-staggered mesh system is employed where the defined positions of velocity and pressure are coincident.

For the temporal integration of the Navier-Stokes equations, the Crank-Nicolson implicit scheme is utilized. This scheme has second-order accuracy in time. These equations and the Poisson equation are iteratively solved at each time step by the successive overrelaxation (SOR) method.

COMPUTATIONAL RESULTS

1) Flow past a circular cylinder

The dependence of the drag coefficients on Reynolds numbers is shown in Fig.3. The number of grid points are 32*16, 64*32, 128*64. If the Reynolds number is less than 100, all the computations and experiments agree very well. At high Reynolds numbers even 64*32 computation can capture the drag crisis qualitatively. The 128*64 computations agrees much better with the experiments as expected.

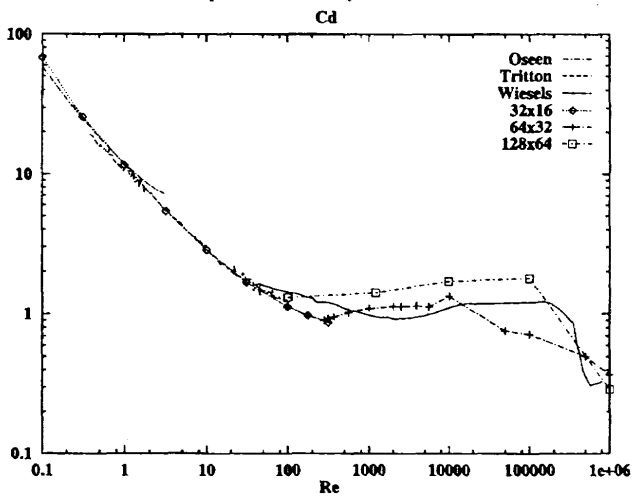

Fig.3 Drag coefficients of circular cylinder

The drag sharply decreases at about Reynolds number 400000, which is called drag crisis, is well captured even using this coarse grid. Instantaneous and time-averaged flow patterns clearly show the difference as shown in Figs. 4-7. After drag crisis, flow separation delays and the wake becomes narrower, which makes the drag less.

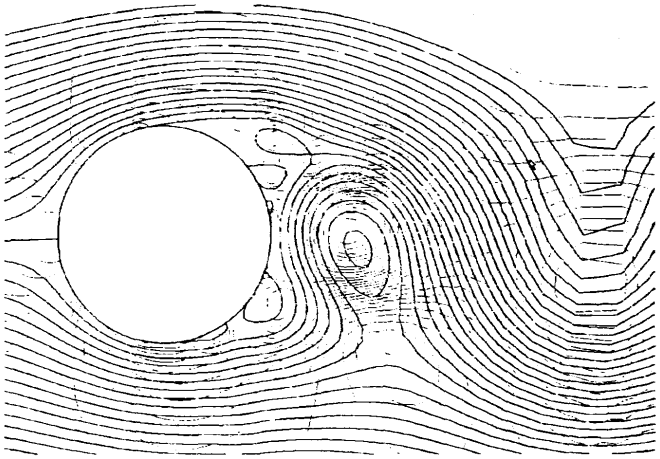

Fig.4 Flow past a circular cylinder at Re=56000, before drag crisis
Streamlines and pressure contours
Instantaneous flow field, 128*64grid

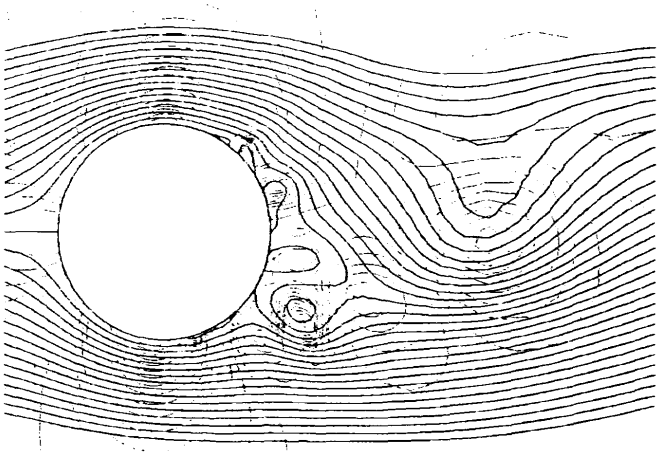

Fig.5 Flow past a circular cylinder at Re=1000000, after drag crisis
Streamlines and pressure contours
Instantaneous flow field, 128*64grid

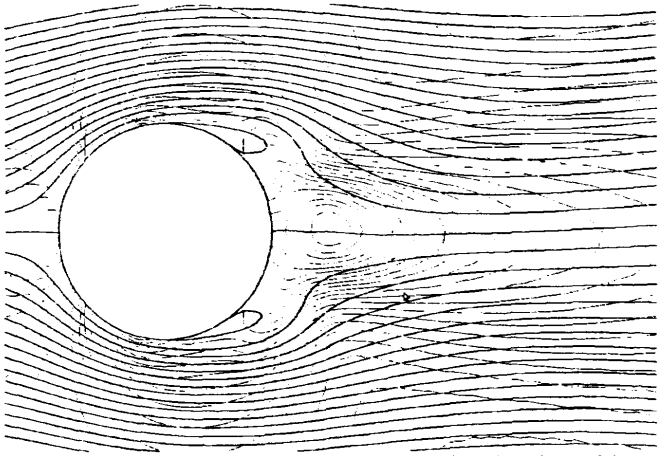

Fig.6 Flow past a circular cylinder at Re=56000, before drag crisis
Streamlines and pressure contours
Time averaged flow field, 128*64grid

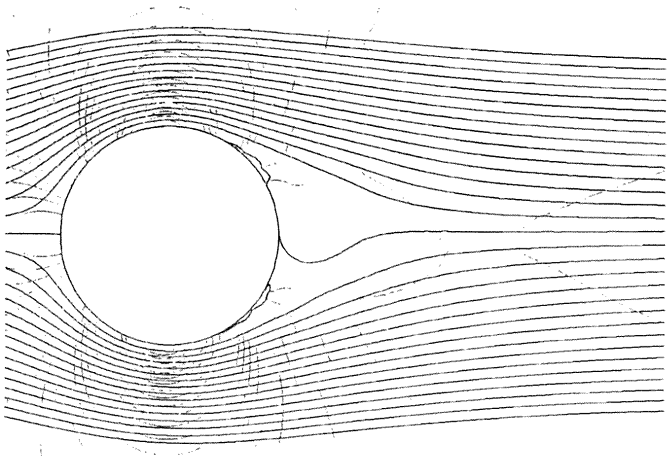

Fig.7 Flow past a circular cylinder at Re=1000000, before drag crisis
Streamlines and pressure contours
Time averaged flow field, 128*64grid

2) Transitional flow in a square channel

It is impossible to compute transitional flow by using turbulence model. Even large-eddy simulation can not handle this type of problem, because it assumes the flow is turbulent from the beginning. However, transition phenomena is very important at high-Reynolds number flow. In the present approach, this is nothing special, we can compute any transitional flow with no special consideration. In Fig.8, development of turbulence behind an obstacle is shown. The visualization was done by showing equi-temperature surface. The temperature at the inlet is only 0.1 degree higher than the initial condition in the channel. This does not affect the computed flow field. However it is very effective for the flow visualization.

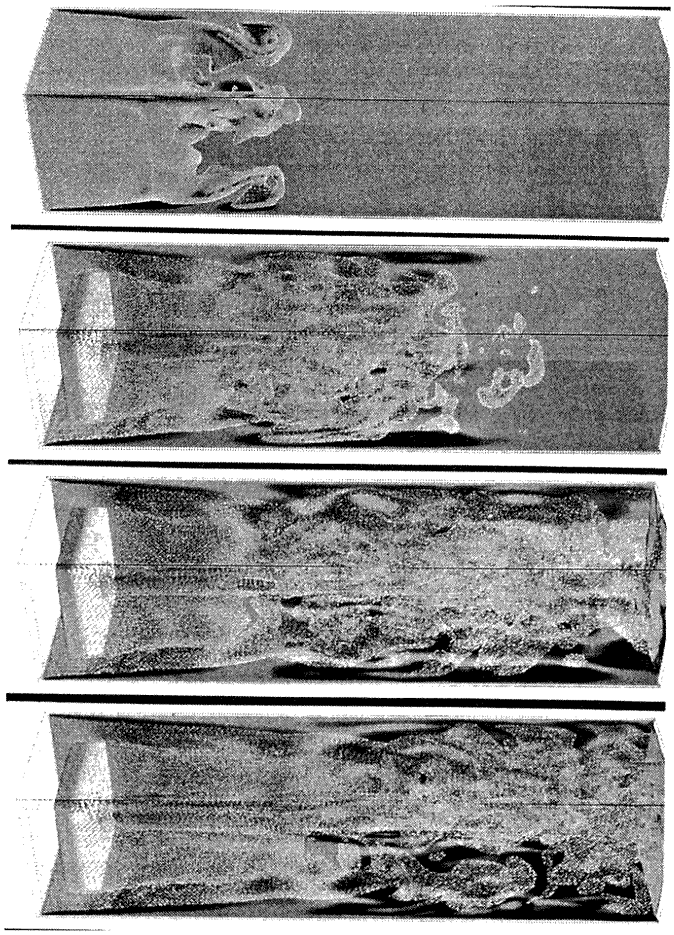

Fig.8 Development of turbulence behind an obstacle
in a square channel at Re=12500, 256*64*64 grid

3) Flow around a car

For car aerodynamics, evaluation of drag and lift coefficients is most important. For this purpose the separation zone should be calculated accurately. At high-Reynolds numbers, as shown in the case of circular cylinder, drag crisis takes place which has decisive effect on the drag. At this moment almost only way which can capture the drag crisis is to use the present upwind method (Fig.9). By using this, drag can be calculated within 5% difference with the experiments (Hashiguchi,1996).

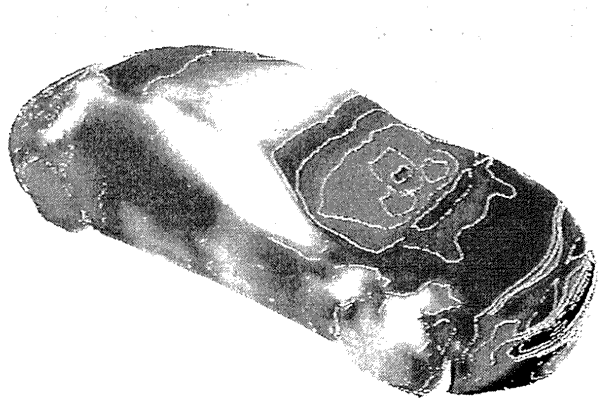

Fig.9 Flow around a car at Re=1000000

4) Thermal convection

Thermal convection is another good example where the transition plays an essential role (Fig.10) (Tsuchiya and Kuwahara 1997). Figure 10 shows equi-temperature surface in the initial stage of the development.

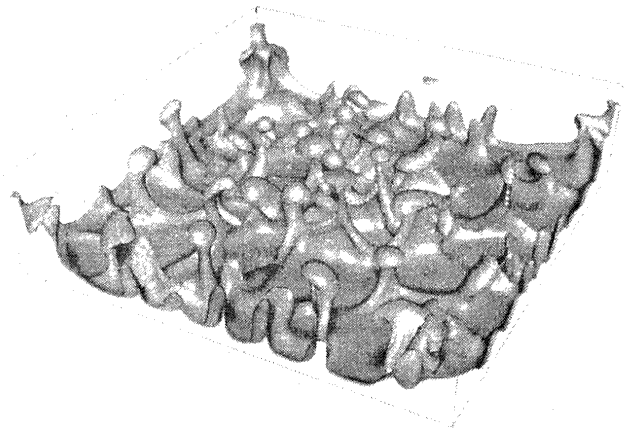

Fig.10 Natural convection in a box heated below,
equi-temperature surface. Rayleigh number 17000000,
128*128*32 grid

VISUALIZATION

The computed data is becoming bigger and bigger and without visualization system understanding of underlying flow mechanism is very difficult. What is needed is a means of properly visualizing the computed flow field. The key points are real-time visualization and animation.

A flow simulation takes a large amount of CPU time, therefore it is desirable to visualize it while computing it. This saves a lot of time especially while debugging. This should be called real-time visualization.

Moreover, a still picture is insufficient when flows become essentially unsteady as those at high Reynolds numbers, since it is impossible to understand the transient flow in total only from a set of instantaneous flow pictures. Visualization by animated graphics is a necessity in this case. Only by using such a system it becomes possible to observe the essentially unsteady flow field and to understand the fundamental flow mechanism underlying it.

The visualization software used here is Globe2D and Globe3D developed by Institute of Computation Fluid Dynamics, which satisfies the above requirements (Kuzuu, Kaizaki, Kuwahara 1997).

CONCLUSIONS

It is becoming clear that we need not resolve the small-scale structure of high-Reynolds-number flow to capture the large structure, which is most important for application. We should not use standard models to

simulate any high-Reynolds-number, turbulent flows. Only without using turbulence models we are able to capture the dependence of the flow on the Reynolds number. To avoid the numerical instability we can simply use a third-order upwind difference. Multi-directional finite-difference makes the dependence of the solution on the flow direction less and the computation more reliable.

ACKNOWLEDGEMENTS

The author would like to thank for the cooperation of Mr. M. Hashiguchi for the case 0 and 1, Dr. K. Kuzuu for case 3 and all of the visualization, Mr. T. Tsuchiya for the case 4.

REFERENCES

Boris, J.P., Grinstein, F.F., Oran, E.S., and Kolbe, R.L., 1992, "New insights into large eddy simulation," Fluid Dynamics Research 10, pp 199-228

Hashiguchi, M., 1996, "Turbulence simulation in the Japanese automotive industry," Engineering Turbulence Modeling and Experiments 3, pp291-308.

Hashiguchi, M., 1997 to appear

Kawamura, T., and Kuwahara, K., 1984, "Computation of high Reynolds number flow around a circular cylinder with surface roughness," AIAA Paper 84-0340.

Kuzuu, K., and Kaizaki, H., and Kuwahara, K., 1997, "Real Time Visualization of Flow Fields Using Open GL System ," AIAA Paper 97-0235.

Kuwahara, K., 1991, "Flow Simulation on Supercomputers and Its Visualization," International Journal of High Speed Computing, Vol.4, No.1, pp49-70.

Tsuchiya, T., and Kuwahara, K., 1997 "Three-Dimensional Computation of Natural Convection in an Enclosure at High Rayleigh Numbers", AIAA Paper 97-0436